



***In Vitro* Studies of Biosynthesized Nanoparticles of *Dysphania* Aqueous Leaves Extract Against Some Isolated Bacteria from Wounds and Burns and *In Silico* Evaluations of Compounds Identified in its GC-MS Spectra**

Ekhlas Q. Jasim¹, Munther A. Muhammad-Ali^{2*}, Amani A. Al-Abdullah³^{1,3} Department of Pathological Analyses, College of Science, Basrah University, Basrah 61001, Iraq² Department of Ecology, College of Science, University of Basrah, Basrah 61001, Iraq**ARTICLE INFO****Article history:**

Received 14 October 2024

Revised 16 October 2024

Accepted 02 November 2024

Published online 01 December 2024

Copyright: © 2024 Jasim *et al.* This is an open-access article distributed under the terms of the [Creative Commons Attribution License](https://creativecommons.org/licenses/by/4.0/), which permits unrestricted use, distribution, and reproduction in any medium, provided the original author and source are credited.

ABSTRACT

Globally, antibacterial resistance is emerging quickly due to various factors. Substitute and more effective medications are essential in the fight against drug-resistant and harmful bacterial species. It has been determined that phytochemicals have great promise in this area. Therefore, considering phytochemicals as a substitute for antibacterial medications can be advantageous. The effectiveness of the silver nanoparticles of *Dysphania ambrosioides* leaf extract was investigated against six strains of pathogenic bacteria isolated from wounds and burns. Additionally, utilising Lipinski's rule of five drug-likeness characteristics, ten bioactive chemicals from *Dysphania ambrosioides* were evaluated for bioactivity in this work. To ascertain their pharmacokinetic actions, ligands with appropriate drug similarity and binding energy comparable to the standard medicines were examined further. The antimicrobial results showed that the concentration of 1000 µg/mL gave effectiveness on some bacterial strains (15 mm against *Staphylococcus aureus*), and the results were compared with some antibiotics (10 mm for vancomycin). The molecular docking of the first ten phytochemicals of the plant extract identified using GC-MS with some active sites of bacterial proteins was studied. It was noted that the best plant component is *If* (1-Octadecanesulphonyl chloride) according to the affinity energy values (-8.10, -8.19, and -8.57 kcal/mol against 3HG7, IJJ and 2RHQ proteins). This investigation revealed phytochemicals with binding energies that were on par with typical medications. Additionally, these compounds were shown to be powerful antibacterial agents by ADME, bioactivity score, and bioavailability radar analysis.

Keywords: *Dysphania ambrosioides*, Silver nanoparticles, Binding affinity, Lipinski's rule, Bioavailability radar analysis

Introduction

Because of their ability to fight bacteria, reduce inflammation, and promote the healing of wounds, silver nanoparticles, or AgNPs, have shown great promise in the medical field. AgNPs have significant antibacterial and antifungal action, which makes them useful for antibacterial coatings, medical implants, and wound dressings. Furthermore, the anti-inflammatory properties of these substances imply possible uses in managing inflammatory ailments, including arthritis. By increasing skin cell proliferation and decreasing inflammation, AgNPs can accelerate wound healing. They can also be used as medication delivery vehicles to enhance therapeutic effects. Their diagnostic uses in biosensors and imaging methods further demonstrate their adaptability in medical diagnostics. Though studies on the safety and effectiveness of AgNPs in clinical settings are ongoing, it is crucial to consider their possible toxicity.^{1,2}

*Corresponding author. E mail: munther.ali@uobasrah.edu.iq
Tel: +9647705615571

Citation: Jasim EQ, Muhammad-Ali MA, Al-Abdullah AA. *In Vitro* Studies of Biosynthesized Nanoparticles of *Dysphania* Aqueous Leaves Extract Against Some Isolated Bacteria from Wounds and Burns and *In Silico* Evaluations of Compounds Identified in its GC-MS Spectra. 2024; 8(11): 9155 – 9165. <https://doi.org/10.26538/tjnpr/v8i11.26>

Official Journal of Natural Product Research Group, Faculty of Pharmacy, University of Benin, Benin City, Nigeria

Many studies have been conducted on the antibacterial activity of silver nanoparticles (AgNPs) from plant extracts. Comparing plant-mediated synthesis to chemically produced AgNPs has several benefits, such as cost-effectiveness, eco-friendliness, and improved biocompatibility.³ For the green synthesis of AgNPs with strong antibacterial properties, a variety of plant extracts, including those from *Azadirachta indica* (neem), *Camellia sinensis* (green tea), *Aloe vera*, *Terminalia arjuna*, and *Cymbopogon citratus* (lemongrass), have been used with success.⁴⁻⁸ These plant-mediated AgNPs are effective against harmful bacteria, such as *Bacillus subtilis*, *Pseudomonas aeruginosa*, *Staphylococcus aureus*, and *Escherichia coli*. According to some researchers^{9,10}, the synergistic effects of the nanoparticles and the bioactive substances found in the plant extracts, such as flavonoids, terpenoids, and phenolic compounds, are responsible for the increased antibacterial activity of these plant-based AgNPs. Plant-mediated AgNPs have a variety of antibacterial mechanisms of action. The nanoparticles' small size and high surface area-to-volume ratio enable them to interact with and pass through bacterial cell membranes, causing harm to the cells and interference with essential cellular processes.¹¹ Furthermore, by interfering with enzyme functions, preventing DNA replication and producing reactive oxygen species that cause oxidative stress in bacterial cells, releasing silver ions (Ag⁺) from the nanoparticles can further enhance their antimicrobial effects.¹² Polyphenols, flavonoids, and terpenoids—bioactive phytochemicals found in plant extracts—can also increase the antibacterial activity of AgNPs. By improving the stability of the nanoparticles, changing their surface characteristics, or displaying their antimicrobial qualities, these phytochemicals can work in concert with the nanoparticles.^{13,14} Gram-positive and Gram-negative bacteria are susceptible to the antibacterial

action of plant-mediated AgNPs, while some research indicates that Gram-negative bacteria are more vulnerable because of their thinner cell walls.^{15,16} Some variables, including the size, shape, concentration, and particular plant extract utilised in the manufacture of the nanoparticles, can affect the antibacterial efficacy of these AgNPs. The green synthesis of AgNPs using plant extracts presents a viable method for creating powerful antibacterial agents that may be used in various industries, such as environmental remediation, food processing, and medicine.^{17,18}

Due to the importance of silver nanoparticles and plant extract, silver nanoparticles were prepared using the green method using the aqueous extract of *Dysphania ambrosioides* leaves. The antibacterial activity of the AgNPs-extract mixture against several bacteria isolated from wounds and burns was studied. *In silico* antibacterial activity of phytochemicals identified in the plant extract using GC-MS was tested against some proteins and compared with standard antibacterial agents.

Materials and Methods

Materials and instruments

AgNO₃ (99.92%, Sigma), Gram stain kit (Titan Biotech. LTD, India), Blood agar (Oxoid, England), MacConkey agar (Oxoid, England), Nutrient agar (Salucea, Netherlands), Incubator (Fisher Scientific, U.S.A), Vitek 2 (Biomerieux, France), Centrifuge (Model PLC-012, Gemmy Instrument Corp., Taiwan), UV-vis spectrophotometer (T80 model, PG Instrument, Ltd., UK), X-Ray Diffraction XRD (Rigaku Ultima IV, Neu-Isenburg, Germany),

Collection and diversity of plant materials

The leaves of *Dysphania ambrosioides* were gathered in the area surrounding the University of Basrah in the city of Basra, Iraq (GPS: [HP7W+VP2](#)) in October 2023. After being chopped into tiny bits, the plant leaves were cleaned with tap or distilled water and allowed to air dry at room temperature in the shade. The dried plant leaves were pulverised using an electric grinder. The powdered plant material was extracted and used in the synthesis of AgNPs.

Green synthesis synthesis of silver particles using aqueous *Dysphania leaf Extracts*.

The extract (10 mL) was added to a beaker containing 0.0242 g of silver nitrate dissolved in 100 mL of distilled water. The mixture was heated at 80 °C for a half hour. After that, sulfone was wrapped around the flask containing the solution to shield it from light and kept in a dark, room-temperature environment for 24 hours. The hue of the solution turned from pale yellow to brown after a day. To separate the AgNPs, the solution was centrifuged at 5,000 rpm for thirty minutes. After isolating at the bottom of the test tubes, the dark solid precipitate was gathered in Petri dishes and thoroughly dried at room temperature.¹⁹

Bacteriological study

Sample collection

A total of 15 wound samples were collected from people of different ages (randomly) from December 2023 to February 2024.

Sample processing

If the area that has to be cleaned is dry, medium was used to moisten the swab. The swab was rotated in a zigzag pattern across the wound surface to collect a sample. It is essential to ensure the swab only touches the wound's surface and not the surrounding skin. The swab was placed back in its plastic wrap (the transport medium) as soon as it had been collected. The sample's name and the date it was taken were written on the label. After that, they were cultivated using a MacConkey medium and blood.

Isolation and Identification of Bacteria

Microscopic examination

The isolates were stained by Gram stain to detect their response to stain, shape, and arrangement.

Colonial morphology on different media

The colonies were grown on a blood agar plate and tested for their shape, size, colour, and blood hemolysis pattern. Meanwhile, those grown on MacConkey agar were tested for their ability to ferment lactose.

Bacteriological identification of bacterial isolates

Microorganisms were identified based on culture traits and gram-staining properties and confirmed with the automated microbiological system vitek2 using gram-positive and gram-negative ID kits.²⁰

Antimicrobial Sensitivity Test

The bacterial isolates were grown overnight, collected using a sterilised inoculating loop, and then mixed with 5 mL of sterile normal saline until the turbidity matched that of the McFarland standard tube. A sterile swab was immersed into the bacterial suspension, and the entire surface of the MHA plate was evenly spread by a swab containing a suspension of bacteria. Sterile forceps were used to pick up the antimicrobial discs and lay them on the inoculated plate's surface. The antibiotic discs were carefully pressed into complete contact with the medium, equally spaced away. Then, the plates were incubated at 37 °C for 24 h. Following incubation, the plates were examined to determine if there were any inhibition zones (clear zones) around the antimicrobial discs, indicating the absence of bacterial growth. The size of the inhibitory zones was interpreted by referencing the standard zone diameter criteria established by the Clinical and Laboratory Standards Institute (CLSI).^{21,22}

Antibacterial Test

Antibacterial activity was measured using Kirby Bauer's agar well diffusion method, which involves preparing nutrient agar plates and spreading 20 µL of the available pathogenic cultures. Using a sterile borer, wells with a diameter of 5 mm were bored. The AgNPs-extract combination was added to wells and distilled water to serve as a control. Standard disc diffusion was employed with antibiotics at 1000 µg/mL. The antibacterial activity of AgNPs-extract of *Dysphania ambrosioides* at 1000 and 500 µg/mL doses was evaluated using an agar well diffusion test. Following that, each plate was incubated at 35°C for 24 h. The inhibition zone was measured millimetres to assess the extract's antibacterial activity against six distinct bacterial strains.²³ The antibacterial activity was replicated three times, and the average diameter of the inhibition zone in millimetres was taken.

GC-MS Analysis

For GC-MS analyses of leaf extracts, the Perkin-Elmer Clarus 680 system (Perkin-Elmer, Inc., U.S.A.) was utilised. It was outfitted with a fused silica column packed with Elite-5MS capillary column (30 m long, 250 µm in diameter, and 0.25 µm thick). The 99.99 percent pure carrier gas was used and pumped at a steady 1 millilitre per minute pace. An electron ionisation energy technique was used for GC-MS spectrum detection using a high ionisation energy of 70 eV (electron Volts), a scan time of 0.2 s, and fragments ranging from 40 to 600 m/z. One litre of injection was made at a split ratio 10:1, with the injector temperature maintained at 250 °C. The column oven temperature was first adjusted to 50 °C for three minutes. After that, it was raised to 280 °C by 10 °C each minute, and finally, it was raised to 300 °C for 10 minutes. The phytochemicals contained in the samples were identified by comparing their mass, peak area, peak height, and retention time (min) spectral patterns with spectral databases of authentic compounds stored in the National Institute of Standards and Technology (NIST) library.

Molecular docking

All ligand and water molecules were removed from the isolated compounds using molecular docking using MOE 2022 v2 Software. The RCSB protein data library provided the crystal structures of D-isomer specific 2-hydroxyacid dehydrogenase (protein ID: 3HG7), *streptococcus pneumoniae* hyaluronate lyase (protein ID: 1C82), *S. aureus* TyrRS (protein ID: 1JJJ), the crystal structure of SpoVG

conserved domain (protein ID: 2I9X) and PheRS from *Staphylococcus haemolyticus*- rational protein (protein ID: 2RHQ). All protein data were obtained from the Protein Data Bank (PDB), available at (<https://www.rcsb.org/>).²⁴⁻²⁶

Rule of Five (RO5)

To assess a compound's drug resemblance and ascertain whether it has the potential to be orally active, drug discovery requires the usage of Lipinski's RO5. The Supercomputing facility for Bioinformatics and Computational Biology (<http://www.scfbio-uitd.res.in/software/drugdesign/lipinski.jsp>) was used in this investigation to screen ligands for the RO5.^{27,28} This analysis was performed on all isolated compounds.

In Silico ADME Analysis

Using SwissADME, pharmacokinetics parameters, including Excretion, Metabolism, Distribution, and Absorption, were assessed in the ligands (<http://www.swissadme.ch/index.php>). The main goal of this assay is to offer information that will aid in developing new drugs.^{29,30}

Ethical Approval

The Human and Animal Ethics Committee at the University of Basrah in Iraq granted approval for all the human interaction techniques detailed in this study (No. 2023/42).

Bioactivity Score and Bioavailability Radar

Using the online Molinspiration program (<http://www.molinspiration.com/>), the bioactivity score of ligands was calculated. This was accomplished using canonical SMILES of ligands acquired from ChemDraw. G-protein coupled receptors (GPCR), kinase inhibitors (KI), nuclear receptor ligands (NRL), enzyme inhibitors (EI), and ion channel modulators (ICM) are among the properties examined. Swiss ADME (<http://www.swissadme.ch/index.php>) identified the ligands bioavailability radar, which provides an instantaneous indication of a compound's oral bioavailability.^{31,32}

Statistical Analysis

Data analysis was conducted using SPSS version 14.0 to assess the bacteria isolation study.

Results and Discussion

By comparing the peak retention time, peak area (percent), peak height (percent), and mass spectral fragmentation patterns of the 60 peaks found in the GC-MS chromatogram of *Dysphania ambrosioides* leaf extracts (Figure 1-A) in aqueous solution to those of the well-known compounds listed in the NIST library bioactive compounds were identified. Table 1 displayed the first ten compounds based on GC-MS data for the extracted media that were recognised as having a decreasing peak area percentage. The first 10 compounds, which were categorised as aliphatic, aromatic, and heterocyclic compounds, were represented by the symbols 1a, 1b, 1c, 1d, 1e, 1f, 1g, 1h, 1i, and 1j, Figure 1-B showed the compounds' structures. Surface plasmon vibrations cause

silver nanoparticles to appear brown in an aqueous media.^{33,34} The UV-vis spectrophotometer was used to confirm the synthesis of silver nanoparticles in sterile distilled water within the wavelength range of 200 to 600 nm. Observing the UV-vis spectrum of the reaction medium made it possible to verify that pure silver ions were reduced to silver nanoparticles when a leaf extract was combined with an aqueous solution of silver ions. Figure 2 displays the UV-Vis absorption spectra of the silver nanoparticles in the leaf extract. The discovery of the silver nanoparticle solution's spectroscopic band at 430 nm validates the process of creating silver nanoparticles.

The synthesised AgNPs' size and crystal structure were demonstrated using an X-ray diffraction spectrometer. At the 100% peak, the AgNPs crystal size rate was measured (Figure 3), with an average crystal volume of 42.34 nm.

In the antibacterial screening, 8 out of 9 bacteria isolated were obtained from patients' wounds. Seven of them were gram-positive, and one isolate was gram-negative. Table 2 shows the results of isolation and diagnosis of bacteria from wounds using the Vitek2 device. The study also revealed that Gram-positive bacteria were more frequent in wounds than Gram-negative bacteria. The difference in isolation rates may be due to people's continuous use of antibiotics and the difference in environments, which affects isolation. The development of people's health awareness plays a role in protecting wounds from infection. There was no significant difference in mean age or sex of patients and the type of isolated bacteria, P value > 0.05. The sensitivity of bacterial isolates to a group of antibiotics was tested using the disc diffusion method. The results in Table 3 showed the diameters of the inhibition zone (mm) and the sensitivity of the bacteria to each antibiotic, estimated according to the Kirby-Bauer method.^{35,36} When conducting antibiotics sensitivity tests, the effect of these antibiotics varied according to each antibiotic by measuring the diameter of the growth inhibition halo obtained. The focus was on the antibiotics used and circulated, which sometimes differ between one used for Gram-positive bacteria and one used for Gram-negative bacteria (Figure 4). The *in vitro* antibacterial activity of the AgNPs-extract of *Dysphania ambrosioides* is presented in Table 4. The combination utilised showed differences in how the six bacterial strains' development was inhibited at two concentrations (1000 and 500 µg/mL). The range of values for the inhibition zone diameter (Figure 5) was between 8 and 17 mm. At concentrations of 1000 and 500 µg/mL, respectively, Table 2 demonstrates that the mixture exhibited the highest efficacy against *Aeromonas salmonicida*, with 15 and 17 mm inhibition zones. On the other hand, *Kocuria kristinae* bacteria exhibit a pronounced resistance to AgNPs-extract at these two concentrations. However, other bacteria were moderately inhibited by the mixture at 1000 µg/mL compared to conventional medications. According to these results, the safety, cost, and broad spectrum of bacteria this type of plant affects make it potentially valuable for treating bacterial resistance to several antibiotics. Because the antibacterial efficacy of medicinal plants is significantly influenced by the phytochemical characteristics of plant families and subfamilies as well as their mode of action.³⁷ These results show that these pathways differ greatly depending on the sorts of components contained in different plant extracts, as indicated by the GC-MS data.

Table 1: Phytochemical compounds of aqueous *Dysphania ambrosioides* extract

Sym.	Peak No.	Name of the compound	Molecular formula	Molecular weight	Peak area (%)	RT (min)
1a	23	2-Methoxy-4-vinylphenol	C ₉ H ₁₀ O ₂	150.18	5.845	15.077
1b	51	Heptadecane	C ₁₇ H ₃₆	240.48	5.4863	19.892
1c	74	Piperine	C ₁₇ H ₁₉ NO ₃	285.34	4.2361	30.520
1d	54	Octadecane	C ₁₈ H ₃₈	254.50	3.5323	20.984
1e	65	Heneicosane	C ₂₁ H ₄₄	296.58	3.4374	23.969
1f	58	1-Octadecanesulphonyl chloride	C ₁₈ H ₃₇ ClO ₂ S	353.00	3.3135	22.029
1g	46	4-Vinylphenol	C ₈ H ₈ O	120.15	3.2808	18.745
1h	70	2-Amino-1,3-propanediol	C ₃ H ₉ NO ₂	91.11	3.0049	27.386
1i	55	Glycine, N, N-dimethyl-, methyl ester	C ₅ H ₁₁ NO ₂	117.15	2.2986	21.047

Table 2: Types of bacteria in clinical samples isolated from wound infection

Bacteria	Gram stain
<i>Staphylococcus aureus</i>	+
<i>Staphylococcus epidermidis</i>	+
<i>Kocuria kristinae</i>	+
Non or low-reactive biopattern	
<i>Staphylococcus aureus</i>	+
<i>Aeromonas salmonicida</i>	-
<i>Granulicatella adiacens</i>	+
<i>Granulicatella adiacens</i>	+
<i>Staphylococcus haemolyticus</i>	+

+ Gram-positive, - Gram-negative

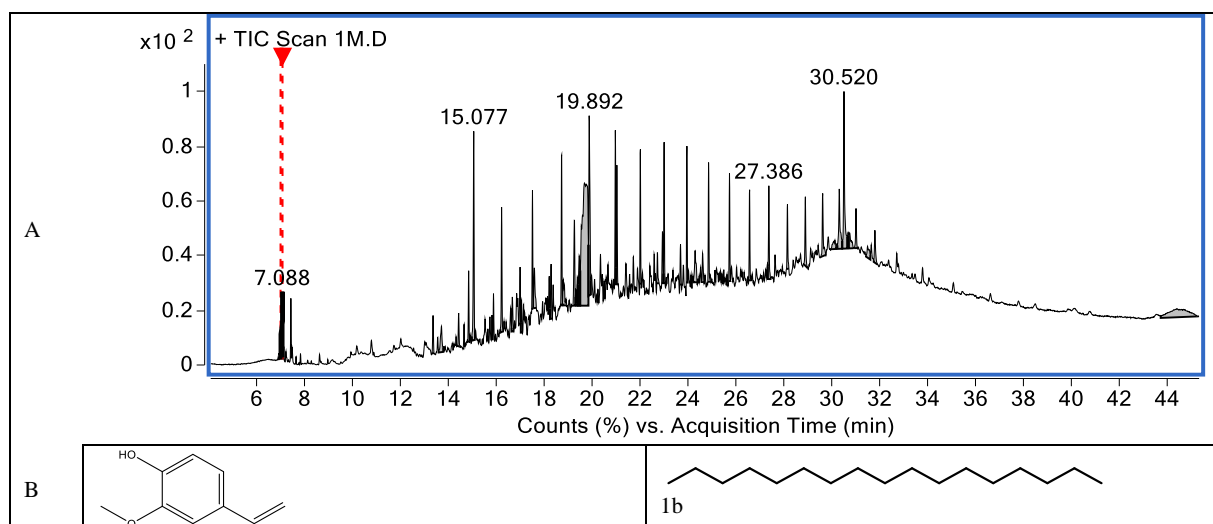
Table 3: Results of Antibiotics sensitivity to bacteria

Bacteria	Inhibition zone (mm)				
	Erythromycin	Ceftriaxone	Vancomycin	Cefoxitin	Ceftazidime
<i>Staphylococcus aureus</i>	22	15	10	8	R
<i>Staphylococcus epidermidis</i>	23	10	10	6	R
<i>Kocuria kristinae</i>	25	13	12	8	R
<i>Staphylococcus aureus</i>	20	13	8	7	R
<i>Aeromonas salmonicida</i>	20	12	10	7	R
<i>Granulicatella adiacens</i> (A)	25	13	12	7	R
<i>Granulicatella adiacens</i> (B)	20	13	11	7	R
<i>Staphylococcus haemolyticus</i>	20	15	11	7	R

Table 4: Inhibition zone of AgNPs-extract against the pathogenic bacterial strains

Tested material	Inhibition Zone (mm)					
	<i>S. aur.</i>	<i>S. epi.</i>	<i>K. kr.</i>	<i>A. sal.</i>	<i>G. ad.</i>	<i>S. ha.</i>
Ag-Ex (1000 µg/mL)	15	12	R	17	11	12
Ag-Ex (500 µg/mL)	12	8	R	15	R	12
E	23	22	24	21	20	21
VA	10	8	8	R	8	10
CTR	15	10	12	13	8	7

Ag-Ex= AgNPs-extract, *S. aur.* = *Staphylococcus aureus*, *S. epi.* = *Staphylococcus epidermidis*, *K. kr.* = *Kocuria kristinae*, *A. sal.* = *Aeromonas salmonicida*, *G. ad.* = *Granulicatella adiacens*, *S. ha.* = *Staphylococcus haemolyticus*, E= Erythromycin, VA= Vancomycin, CTR= Ceftriaxone, R= No inhibition



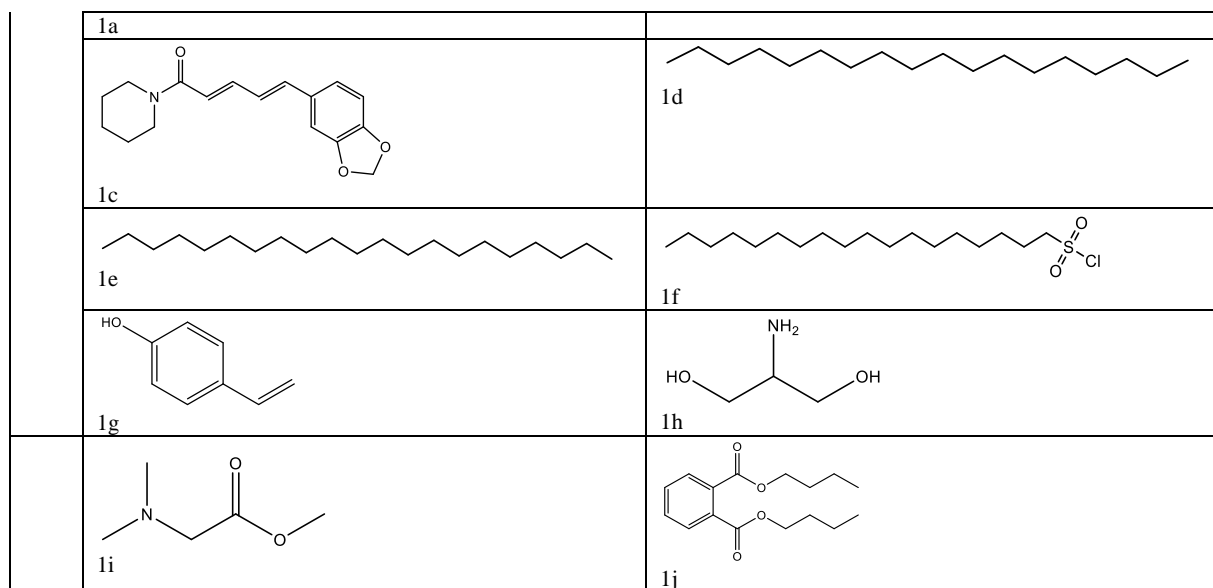


Figure 1: (A) GC-MS chromatogram of *Dysphania ambrosioides* leaf extract. (B) Chemical structures of the first ten phytochemicals.

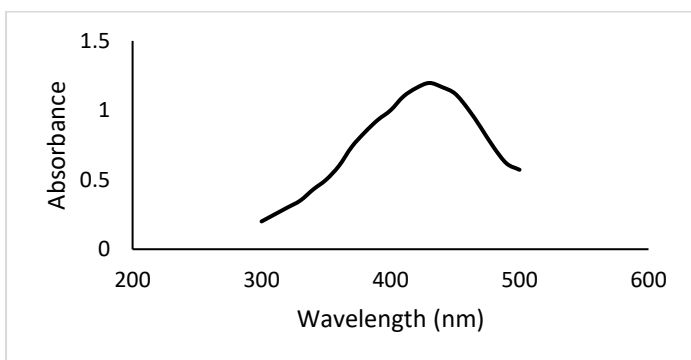


Figure 2: UV-Vis. Spectrum of silver nanoparticles

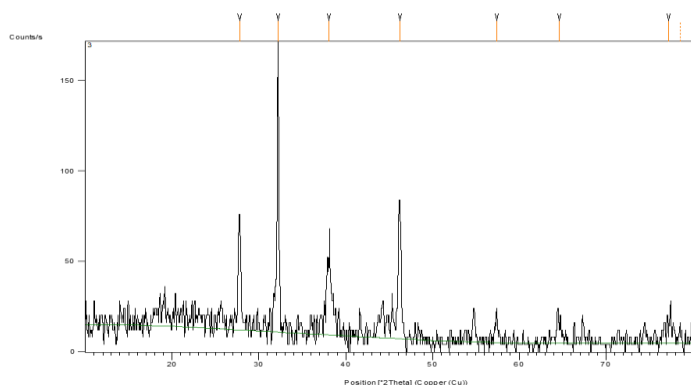


Figure 3: XRD pattern of AgNPs

Based on the minimum binding score and RMSD values, the top ten phytochemicals (1a, 1b, 1c, 1d, 1e, 1f, 1g, 1h, 1i, and 1j) with the highest concentrations as determined by GC-MS analysis were tested individually against each receptor protein of the chosen bacteria (Table 5). The docking or binding-free energy, which denotes the binding affinity of these 10 ligands and the three prescription drugs, has been determined, as shown in Table 5 and Figures 6 and 7. Out of ten phytochemicals, 1f exhibits the maximum binding affinity of -8.10 , -5.83 , -8.19 , -6.00 , and -8.57 kcal/mol against 3HG7, 1C82, 1JJJ, 2I9X, and 2RHQ, respectively. In comparison, 1h has the lowest affinity among the ten phytochemicals in the -3.83 to -4.60 kcal/mol range against the same proteins. Several tested phytochemical ligands were found to have binding energies that were either higher or equal to

those of the prescription medications. At least one protein from each of the five protein classes is displayed in Figure 8, along with the improved docking energy, surface, and poses views of phytochemical ligand 1f. The binding affinity values between the phytochemicals and the proteins under investigation led us to conclude that the ligands had a higher affinity for the active sites of the proteins 2RHQ and 1JJJ than the other proteins (Table 5). 1-Octadecanesulphonyl chloride (1f) was shown to bind with the 3HG7 protein's SER284 and TYR75 amino acids with interaction types of H-acceptor and H-pi, respectively, giving ligand stability with the active site of high value -44.87 kcal/mol (Table 6).^{38,39} The 1C82 protein was shown to have a standard H-acceptor with ASP629, providing ligand stability of -27.45 kcal/mol. Conversely, post-site amino acids TYR36, LEU8, and GLY315 of 1JJJ, 2I9X, and 2RHQ proteins were shown to have H-acceptor interactions, with ligand stability of -33.75 , -30.31 , and -39.35 kcal/mol, respectively. In the binding domain of the 3HG7 protein, Table 6 demonstrates how various phytochemicals interacted with ALA76 and HIS279 as a common H-acceptor interacting residue. The amino acids HIS578, ASP629, and LYS581 were found to be frequently involved in many interactions (H-acceptor, H-pi, H-donor, and ionic) of the 1C82 protein. In contrast, protein 1JJJ provided dominating H-interactions by ASP177 amino acid with ligands, followed by TYR36 and GLY193. The phytochemical interacted with the active pocket amino acids LYS78, THR4, VAL6, and LEU8 in the 2I9X target protein. Additionally, two types of interference with distinct H-bonding were seen for the amino acids GLU216, PHE254, and PHE256 in the 2RHQ protein's active region (Table 7).

The Derwent Word Drug Index (WDI), Modern Drug Data Report (MDDR), and Comprehensive Medicinal Chemistry (CMC) are the most popular methods of drug-like data sets.⁴⁰ The term "drug-like" has several meanings depending on how it is administered. The Lipinski rule of five verified characteristics, namely molecular weight, hydrogen donor, hydrogen acceptor, lipophilicity, and molar refractivity, was used to screen the drug qualities of the chosen phytochemicals.⁴¹ Ninety percent of orally active medications that have reached the phase II clinical stage fall into one of four simple physicochemical parameter ranges (MWT ≤ 500 , $\log P \leq 5$, H-bond donors ≤ 5 , H-bond acceptors ≤ 10) that were defined in the original RO5 which deals with compounds that are orally active.⁴² All five of Lipinski's criteria were met by 1a, 1b, 1c, 1d, 1e, 1f, 1g, 1h, 1i, and 1j; 1f failed the criterion ($\text{LOGP} = 9.56$), while the other ones just deviated in one or two of the criteria, which is still acceptable (Table 8). Oral bioavailability begins with these physicochemical properties linked to intestinal permeability and appropriate aqueous solubility. A chemical has a high likelihood of causing oral activity issues if it fails the RO5. A chemical is not always drug-like just because it passes the RO5.⁴³

The drugability qualities of ligands such as GPCR ligand, protease inhibitor (PI), kinase inhibitor (KI), nuclear receptor ligand (NRL), ion channel modulator (ICM), and enzyme inhibitor (EI) were determined by the bioactivity score. The ligand scores were predicted using the Molinspiration web service. A score of more than 0.00 indicates strong activity, a number between -0.5 and -0.00 indicates moderate activity, and a score below -0.5 suggests inactivity.^{44,45} Table 9 displays that all of the phytochemicals under investigation exhibited good scores of high to moderate activity, except for *Ig*, *Ih*, and *Ii*, which displayed inactivity in all parameters. On the other hand, *Ia* demonstrated activity for ICM and EI (-0.28 and -0.046, respectively). Compounds *Ie* and *If* had the most potent bioactivity compared to other phytochemicals. High

bioactivity scores indicated the potential for these bioactivities as powerful therapeutic agents; the higher the scores, the better the activity.⁴⁶

Similarly, the bioavailability radar offers a quick evaluation of a compound's drug-likeness. As shown in Figure 9, the pink area represents the ideal range for each parameter. A phytochemical's radar plot must fall within this range for it to be deemed drug-like; as a result, the radar plot predicts whether or not the ligands will be orally bioavailable.^{47,48} It is possible to indicate that four phytochemicals under study, *Ic*, *Ih*, *Ii*, and *Ij*, are orally accessible since they meet the radar plot criteria.

Table 5: Docking scores of phytochemicals compounds and standard drugs covalently bound to the active site of D-isomer specific 2-hydroxyacid dehydrogenase (protein ID: 3HG7), *streptococcus pneumoniae* hyaluronate lyase (protein ID: 1C82), *S. aureus* TyrRS (protein ID: 1JJJ), crystal structure of SpoVG conserved domain (protein ID: 2I9X) and PheRS from *Staphylococcus haemolyticus*-rational protein (protein ID: 2RHQ)

Compound	Docking affinity (kcal/mol)									
	3HG7	RMSD Å	1C82	RMSD Å	1JJJ	RMSD Å	2I9X	RMSD Å	2RHQ	RMSD Å
<i>Ia</i>	-4.71	1.02	-4.27	2.71	-5.42	1.54	-4.18	2.37	-5.04	1.36
<i>Ib</i>	-6.99	1.67	-4.91	2.01	-7.07	2.11	-5.67	2.27	-7.28	1.79
<i>Ic</i>	-6.97	1.61	-5.28	1.74	-6.88	1.85	-5.42	1.50	-6.81	1.06
<i>Id</i>	-7.02	1.56	-5.16	1.42	-7.39	2.33	-5.95	1.65	-7.46	2.10
<i>Ie</i>	-7.76	1.93	-5.66	2.15	-7.89	1.77	-5.80	2.36	-8.42	2.34
<i>If</i>	-8.10	1.23	-5.83	1.95	-8.19	2.35	-6.00	2.00	-8.57	1.68
<i>Ig</i>	-4.34	1.68	-3.82	1.67	-4.70	1.21	-3.94	1.56	-4.49	1.50
<i>Ih</i>	-3.83	1.90	-3.40	2.36	-4.60	2.11	-3.44	1.75	-4.23	1.58
<i>Ii</i>	-4.49	2.04	-4.14	1.09	-4.74	1.96	-4.21	1.58	-4.94	2.60
<i>Ij</i>	-6.63	1.48	-5.17	2.66	-7.06	1.46	-5.27	1.52	-6.54	1.79
Ceftriaxone	-9.25	2.05	-7.22	2.49	-8.85	2.08	-6.13	2.08	-8.24	1.64
Erythromycin	-8.50	2.33	-5.84	1.91	-8.64	2.47	-6.02	1.61	-8.62	2.11
Vancomycin	-11.42	2.70	-8.72	1.98	-11.68	2.01	-7.28	1.84	-9.03	2.62

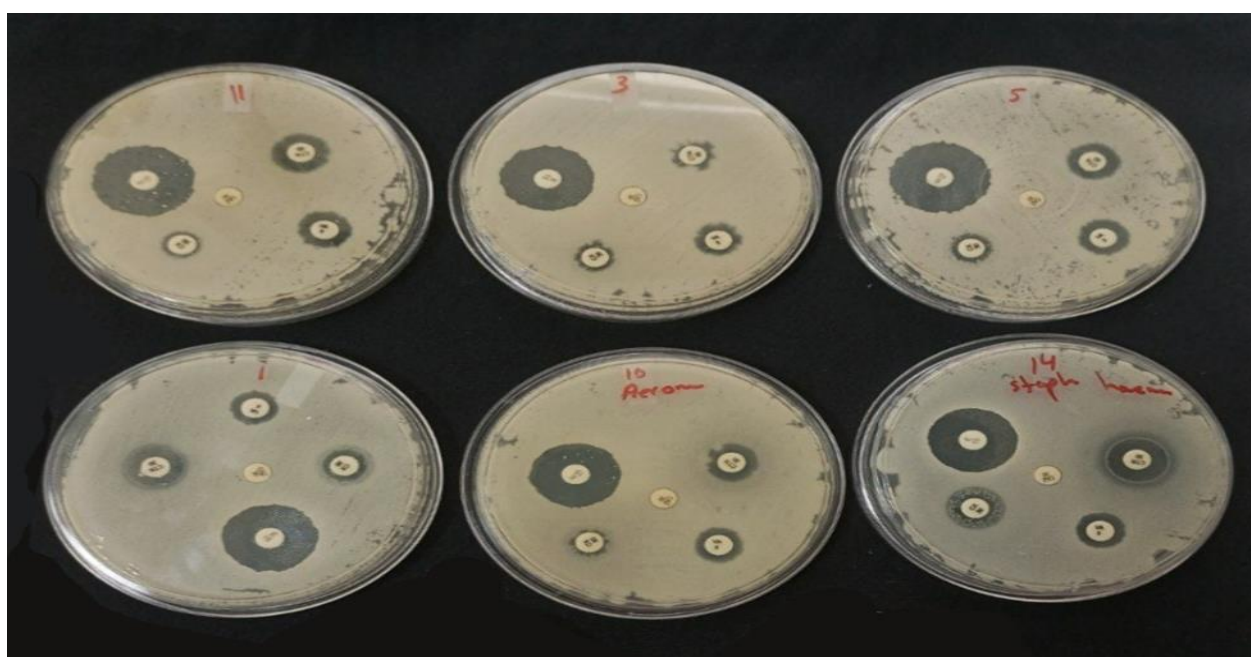


Figure 4: Antibiotic sensitivity of bacteria isolation from wound infection

Table 6: The binding data of phytochemicals *1a*, *1b*, *1c*, *1d*, *1e*, *1f*, *1g*, *1h*, *1i*, and *1j* against proteins 3HG7, 1C82, and 1JJJ

Compd.	Bonds between Atoms of Compounds and Residues of Active Site											
	3HG7				1C82				1JJJ			
	Receptor (Interaction)	Residues	Distance (Å)	Stability of ligand (kcal/mol)	Receptor (Interaction)	Residues	Distance (Å)	Stability of ligand (kcal/mol)	Receptor (Interaction)	Residues	Distance (Å)	Stability of ligand (kcal/mol)
<i>1a</i>	SER 281 (H-donor)		2.99	-21.13	GLU 768 (H-donor)		2.96	-21.87	ASP 177 (H-donor)		2.99	-22.80
<i>1b</i>	HIS 279 (H-pi)		3.87	-34.71				-22.65				-29.87
<i>1c</i>	ALA 282 (H-acceptor)		2.95	-38.75	HIS 578 (H-pi)		3.82	-25.68	ASP 177 (H-donor)		3.11	-33.52
<i>1d</i>				-37.04				-23.55	GLY 193 (H-acceptor)		2.92	-33.26
<i>1e</i>	TYR 75 (H-pi)		4.24	-43.18				-28.70				-32.42
<i>1f</i>	SER 284 (H-acceptor)		3.10	-44.87	ASP 629 (H-acceptor)		3.06	-27.45	TYR 36 (H-acceptor)		2.71	-33.75
<i>1g</i>	TYR 75 (H-pi)		4.38		GLU 768 (H-donor)		2.87	-16.38	ASP 177 (H-donor)		2.86	-22.03
<i>1h</i>	SER 281 (H-donor)		3.05	-18.42	LYS 581 (pi-cation)		4.75		ASP 177 (H-donor)		2.89	
	SER 284 (H-donor)		3.30	-15.80	ASP 629 (H-donor)		3.14		TYR 36 (H-acceptor)		3.21	-21.38
	ALA 76 (H-acceptor)		3.21		NA 908 (Metal)		2.81	-13.45	ASP 177 (Ionic)		3.05	
<i>1i</i>					ASP 629 (Ionic)		3.14					
	HIS 279 (H-acceptor)		3.05	-21.84	LYS 581 (H-acceptor)		3.51					
	ALA 76 (H-acceptor)		3.03		HIS 578 (H-acceptor)		3.02	-22.87				-22.65
					NA 906 (Metal)		2.55					
<i>1j</i>	ALA 76 (H-acceptor)		3.12		LYS 581 (H-acceptor)		3.24		CYS 37 (H-donor)		3.73	
	GLY 77 (H-acceptor)		3.05	-36.28			2.90	-28.78	GLY 193 (H-acceptor)		3.37	-36.10
	HIS 279 (H-acceptor)		3.09		HIS 578 (H-acceptor)		2.55		HIS 50 (H-pi)		4.02	
					NA 906 (Metal)							

Table 7: The binding data of phytochemicals *1a*, *1b*, *1c*, *1d*, *1e*, *1f*, *1g*, *1h*, *1i*, and *1j* against proteins 2I9X and 2RHQ

Compound	Bonds between Atoms of Compounds and Residues of Active Site									
	2I9X					2RHQ				
	Receptor (Interaction)	Residues	Distance (Å)	Stability of ligand (kcal/mol)	Receptor (Interaction)	Residues	Distance (Å)	Stability of ligand (kcal/mol)		
<i>1a</i>	THR 4 (H-donor)		2.94	-17.66	PHE 254 (H-pi)		3.95	-22.83		
<i>1b</i>	VAL 6 (pi-H)		4.00	-27.93	PHE 256 (pi-H)		3.71	-31.62		
<i>1c</i>					GLU 216 (H-donor)		3.31			
<i>1d</i>	LEU 8 (H-donor)		3.29	-27.97	PHE 254 (H-pi)		3.81	-27.29		
<i>1e</i>				-28.95	PHE 256 (pi-H)		4.36	-28.88		
<i>1f</i>				-29.14				-34.71		
<i>1g</i>	LEU 8 (H-acceptor)		3.03	-30.31	GLY 315 (H-acceptor)		2.98	-39.85		
<i>1h</i>	LYS 78 (pi-cation)		4.18	-15.0	PHE 254 (H-pi)		4.09	-20.51		
<i>1i</i>					PHE 256 (pi-H)		3.95			
<i>1j</i>	ALA 75 (H-donor)		3.08	-10.37	GLU 216 (H-donor)		2.97	-15.83		
	THR 4 (H-donor)		2.96		GLU 216 (Ionic)		2.97			
	LYS 78 (H-acceptor)		3.31	-20.10						
	VAL 6 (H-acceptor)		2.92		GLN 177 (H-acceptor)		3.12	-18.99		
	LYS 78 (pi-cation)		3.79	-24.77	GLN 214 (H-acceptor)		3.01	-35.07		

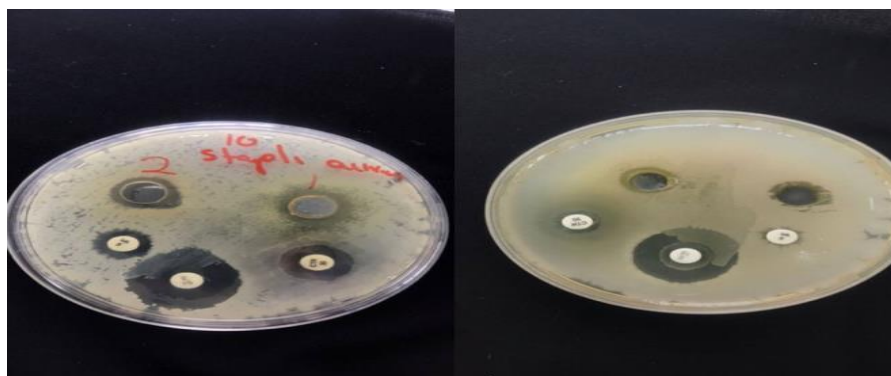
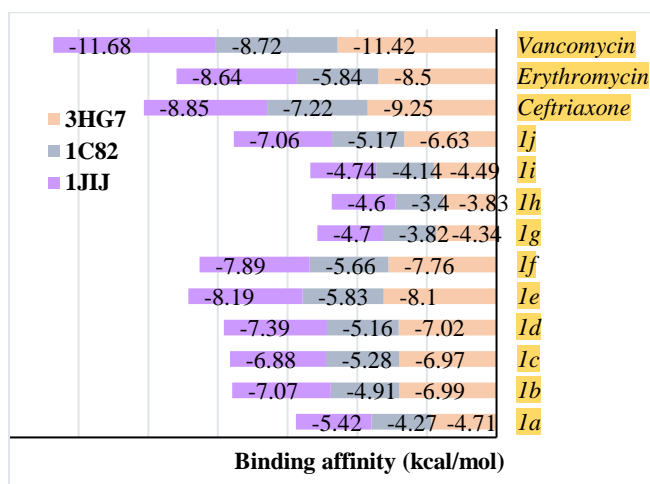
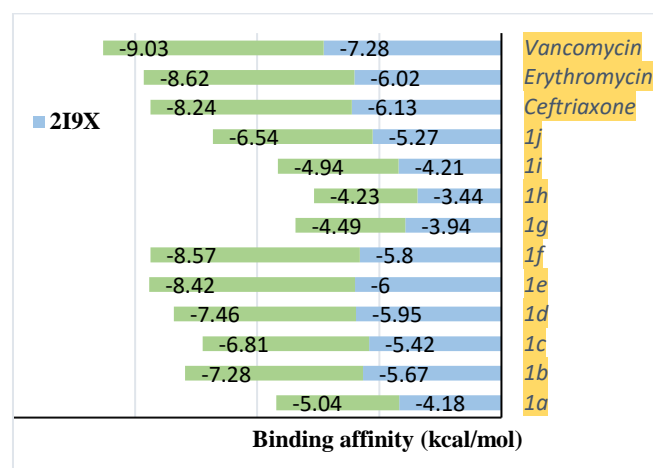
Table 8: Lipinski's rule of five

Phytochemicals	Mass	Hydrogen bond donor	Hydrogen bond acceptor	LOGP	Molar refractivity
<i>1a</i>	150	1	2	0.88	42.83
<i>1b</i>	240	0	0	4.30	171.87
<i>1c</i>	285	0	4	-1.52	86.67
<i>1d</i>	254	0	0	4.55	181.60
<i>1e</i>	296	0	0	5.28	210.79
<i>1f</i>	352.5	1	2	9.56	322.55
<i>1g</i>	120	0	1	-1.32	30.55
<i>1h</i>	91	0	3	-1.84	23.17

<i>li</i>	117	1	2	2.30	36.63
<i>lj</i>	278	0	4	5.22	86.17

Table 9: Compounds' bioactivity score using Molinspiration.com

Compd.	GPCR	ICM	KI	NRL	PI	EI
<i>la</i>	-0.96	-0.28	-1.00	-0.77	-1.34	-0.46
<i>lb</i>	-0.21	-0.01	-0.34	-0.25	-0.31	-0.04
<i>lc</i>	0.15	-0.18	-0.13	-0.13	-0.10	0.04
<i>ld</i>	-0.09	0.00	-0.19	-0.10	-0.17	0.02
<i>le</i>	0.02	0.00	-0.07	0.02	-0.02	0.03
<i>lf</i>	0.03	-0.08	-0.17	0.00	0.01	0.04
<i>lg</i>	-2.08	-1.19	-2.21	-1.76	-2.43	-1.52
<i>lh</i>	-2.97	-3.29	-3.02	-3.66	-2.68	-3.07
<i>li</i>	-3.11	-2.75	-3.51	-3.41	-3.08	-2.95
<i>lj</i>	-0.07	-0.08	-0.19	-0.03	-0.13	-0.04

**Figure 5:** Inhibition zone (mm) of AgNPs-extract and standard drugs against bacterial isolates A- *Staphylococcus aureus* B- *Staphylococcus epidermidis***Figure 6:** Binding scores of phytochemicals and standard drugs against 3HG7, 1C82, and 1JJJ proteins**Figure 7:** Binding scores of phytochemicals and standard drugs against 2I9X and 2RHQ proteins

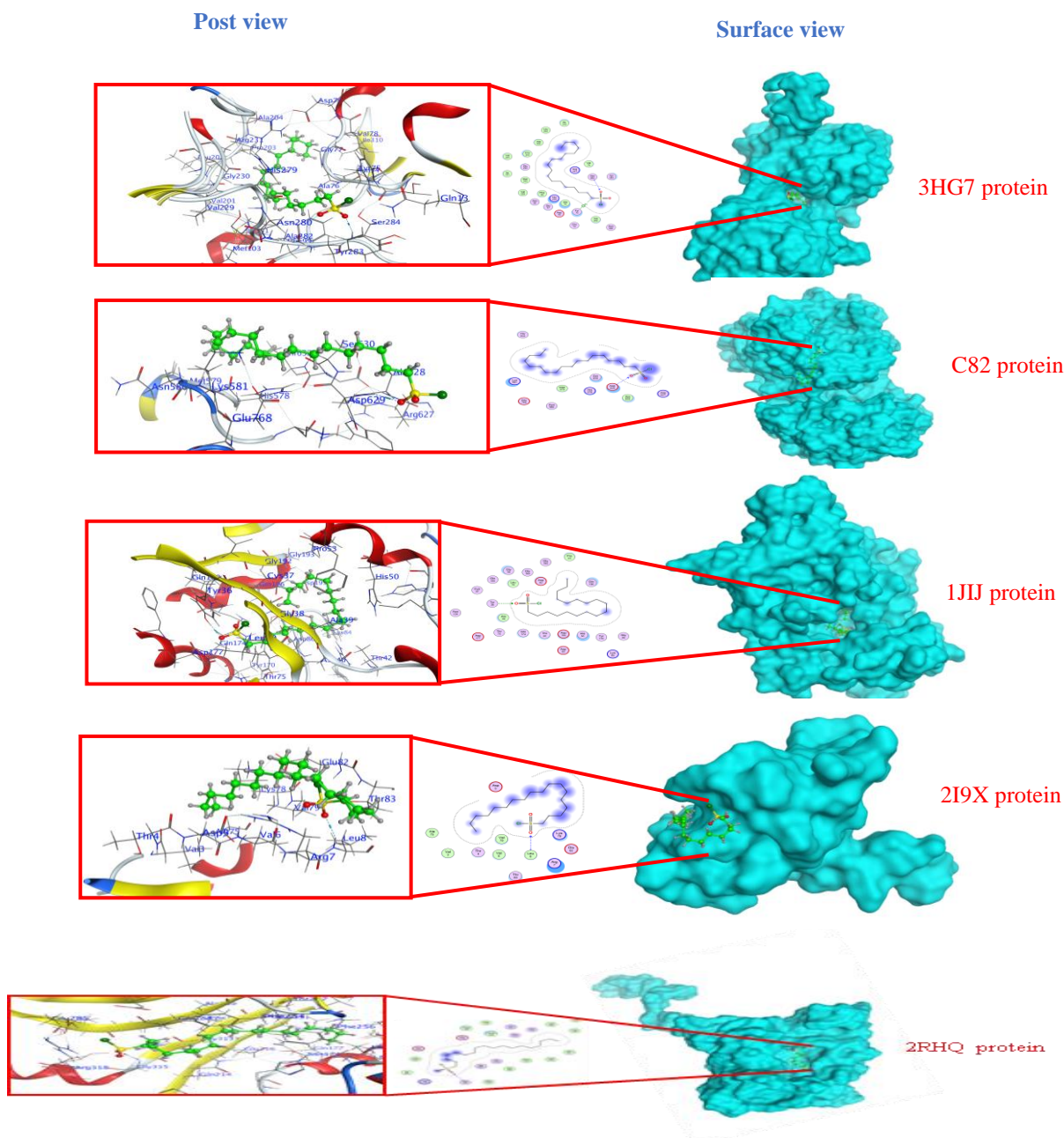


Figure 8: Different binding modes of *l* within the active and catalytic sites of five selected proteins

Conclusion

The potential of different phytochemicals to inhibit bacterial growth is investigated using *in vitro* and molecular docking studies, which also compare the theoretical and empirical antibacterial evaluation of nanoparticles containing phytochemicals and conventional medications. According to our data, four phytochemicals, 1c, 1h, 1i, and 1j, had pharmacokinetic activity and similarity equal to conventional drugs. This indicates that bioactive substances can prevent the growth of bacteria. More research is required to determine the pharmacodynamics and kinetic characteristics of these phytochemicals and to examine the toxicity of the plant extract and AgNPs-extract mixture. The antibacterial activity was observed to be good using the combination of nanoparticles and plant extract, which opens future horizons for developing other types of plant extracts and other nanoparticles.

Conflict of Interest

The authors declare no conflict of interest.

Authors' Declaration

The authors hereby declare that the work presented in this article is original and that any liability for claims relating to the content of this article will be borne by them.

References

- Gamboa SM, Rojas ER, Martínez VV, Vega-Baudrit J. Synthesis and characterisation of silver nanoparticles and their application as an antibacterial agent. *Int. J. Biosen. Bioelectron.* 2019; 5(5):166-173. <https://doi.org/10.15406/ijbsbe.2019.05.00172>

2. Durán N, Durán M, De Jesus MB, Seabra AB, Fávoro WJ, Nakazato G. Silver nanoparticles: A new view on mechanistic aspects of antimicrobial activity. *Nanomed.: Nanotechn., Bio. Med.* 2016; 12(3):789-799. <https://doi.org/10.1016/j.nano.2015.11.016>
3. Tailor G, Yadav BL, Chaudhary J, Joshi M, Suvalka C. Green synthesis of silver nanoparticles using *Ocimum canum* and their antibacterial activity. *Biochem. Biophys. Rep.* 2020; 24:100848. <https://doi.org/10.1016/j.bbrep.2020.100848>
4. Arsene MM, Viktorovna PI, Alla M, Mariya M, Davares AK, Carime BZ, Anatolievna GO, Vyacheslavovna YN, Vladimirovna ZA, Andreevna SL, Aleksandrovna VE. Antimicrobial activity of phytofabricated silver nanoparticles using *Carica papaya L.* against Gram-negative bacteria. *Vet. World.* 2023; 16(6):1301. <https://doi.org/10.14202/vetworld.2023.1301-1311>
5. Cardoso-Avila PE, Patakfalvi R, Rodríguez-Pedroza C, Aparicio-Fernández X, Loza-Cornejo S, Villa-Cruz V, Martínez-Cano E. One-pot green synthesis of gold and silver nanoparticles using *Rosa canina L.* extract. *RSC advances.* 2021; 11(24):14624-14631. <https://doi.org/10.1039/d1ra01448j>
6. Bhat RS, Almusallam J, Al Daihan S, Al-Dbass A. Biosynthesis of silver nanoparticles using *Azadirachta indica* leaves: characterisation and impact on *Staphylococcus aureus* growth and glutathione-S-transferase activity. *IET Nanobiotech.* 2019; 13(5):498-502. <https://doi.org/10.1049/iet-nbt.2018.5133>
7. Gupta A, Briffa SM, Swingler S, Gibson H, Kannappan V, Adamus G, Kowalczyk M, Martin C, Radecka I. Synthesis of silver nanoparticles using curcumin-cyclodextrins loaded into bacteria cellulose-based hydrogels for wound dressing applications. *Biomacromol.* 2020; 21(5):1802-1811. <https://doi.org/10.1021/acs.biomac.9b01724>
8. Liaqat N, Jahan N, Anwar T, Qureshi H. Green synthesised silver nanoparticles: Optimisation, characterisation, antimicrobial activity, and cytotoxicity study by hemolysis assay. *Front. Chem.* 2022; 10:952006. <https://doi.org/10.3389/fchem.2022.952006>
9. Singh P, Kim YJ, Zhang D, Yang DC. Biological synthesis of nanoparticles from plants and microorganisms. *Trends Biotechnol.* 2016; 34(7):588-599. <https://doi.org/10.1016/j.tibtech.2016.02.006>
10. Antunes Filho S, Dos Santos MS, Dos Santos OA, Backx BP, Soran ML, Oprüş O, Lung I, Stegarescu A, Bououdina M. Biosynthesis of nanoparticles using plant extracts and essential oils. *Molecules.* 2023; 28(7):3060. <https://doi.org/10.3390/molecules28073060>
11. Bruna T, Maldonado-Bravo F, Jara P, Caro N. Silver nanoparticles and their antibacterial applications. *Inter. J. Mol. Sci.* 2021; 22(13):7202. <https://doi.org/10.3390/ijms22137202>
12. Loo YY, Rukayadi Y, Nor-Khaizura MA, Kuan CH, Chieng BW, Nishibuchi M, Radu S. In vitro antimicrobial activity of green synthesised silver nanoparticles against selected gram-negative foodborne pathogens. *Front. Microbio.* 2018; 9:1555. <https://doi.org/10.3389/fmicb.2018.01555>
13. Su C, Huang K, Li HH, Lu YG, Zheng DL. Antibacterial properties of functionalised gold nanoparticles and their application in oral biology. *J. Nanomat.* 2020; 2020(1):5616379. <https://doi.org/10.1155/2020/5616379>
14. Harish V, Tewari D, Gaur M, Yadav AB, Swaroop S, Bechelany M, Barhoum A. Review on nanoparticles and nanostructured materials: Bioimaging, biosensing, drug delivery, tissue engineering, antimicrobial, and agro-food applications. *Nanomat.* 2022; 12(3):457. <https://doi.org/10.3390/nano12030457>
15. Rai MK, Deshmukh SD, Ingle AP, Gade AK. Silver nanoparticles: the powerful nano weapon against multidrug-resistant bacteria. *J. Appl. Microbio.* 2012; 112(5):841-852. <https://doi.org/10.1111/j.1365-2672.2012.05253.x>
16. Zargar M, Hamid AA, Bakar FA, Shamsudin MN, Shameli K, Jahanshiri F, Farahani F. Green synthesis and antibacterial effect of silver nanoparticles using *Vitex negundo L.* *Molecules.* 2011; 16(8):6667-6676. <https://doi.org/10.3390/molecules16086667>
17. Naveed M, Bukhari B, Aziz T, Zaib S, Mansoor MA, Khan AA, Shahzad M, Dablood AS, Alruways MW, Almalki AA, Alamri AS. Green synthesis of silver nanoparticles using the plant extract of *Acer oblongifolium* and study of its antibacterial and antiproliferative activity via mathematical approaches. *Molecules.* 2022; 27(13):4226. <https://doi.org/10.3390/molecules27134226>
18. Lakkim V, Reddy MC, Pallavali RR, Reddy KR, Reddy CV, Inamuddin, Bilgrami AL, Lomada D. Green synthesis of silver nanoparticles and evaluation of their antibacterial activity against multidrug-resistant bacteria and wound healing efficacy using a murine model. *Antibiotics.* 2020; 9(12):902. <https://doi.org/10.3390/antibiotics9120902>
19. Daish MK, Muhammad-Ali MA, Al-Asadi WM. Green Synthesis of Nanoparticles Using Aqueous Leaves Extract of *Capparis spinosa L.* and Evaluation of their Resistance to Salt Stress of some Aquatic Plants. *IOP Conf. Ser.: Ear. Envi. Sci.* 2024; 1371(2):022003. <https://doi.org/10.1088/1755-1315/1371/2/022003>
20. Hamzah AF, Abd-alsahib WH, Mahdi SS. Isolation and identification of new bacterial strains isolated from different sources of Al-Rafidiyah oil field in Iraq. *Catrina: Inter. J. Envi. Sci.* 2020; 21(1):15-22. <https://doi.org/10.21608/cat.2020.23299.1041>
21. Benkova M, Soukup O, Marek J. Antimicrobial susceptibility testing: currently used methods and devices and the near future in clinical practice. *J. Appl. microbio.* 2020; 129(4):806-822. <https://doi.org/10.1111/jam.14704>
22. Bashir M, Isa H, Chimbekujwo K, Kachalla NA, Umar AB, Bilyaminu M. Antibiotic sensitivity profile of bacteria isolated from urinary catheters in urinary tract infections patients. *Micro. Infect. Dis.* 2021; 2(4):706-714. <https://doi.org/10.21608/MID.2020.44217.1067>
23. Jasim EQ, Muhammad-Ali MA, Almakki A. Synthesis, characterisation, and antibacterial activity of some mesalazine derivatives. *Sci. Tech. Ind.* 2023; 8(3):338-343. <https://doi.org/10.26554/sti.2023.8.3.338-343>
24. Vavra O, Filipovic J, Plhak J, Bednar D, Marques SM, Brezovsky J, Stourac J, Matyska L, Damborsky J. CaverDock: a molecular docking-based tool to analyse ligand transport through protein tunnels and channels. *Bioinformatics.* 2019; 35(23):4986-4993. <https://doi.org/10.1093/bioinformatics/btz386>
25. Azeez S, Alhashim ZG, Al Otaibi WM, Alsuwat HS, Ibrahim AM, Almandil NB, Borgio JF. State-of-the-art tools to identify druggable protein ligands of SARS-CoV-2. *Arch. Med. Sci.* 2020; 16(1). <https://doi.org/10.5114/aoms.2020.94046>
26. Otuokere IE, Akoh OU, Echeme JO, Nwadike FC, Nwankwo CI, Egbucha JN, Ammasai K. GC-MS Analysis and Molecular Docking Studies to Identify Potential SARS-CoV-2 Nonstructural Protein Inhibitors from *Icacina trichantha* Oliv Tubers. *Trop J. Pharm Res.* 2022; 6(8):1336-1342. <https://doi.org/10.26538/tjnpr/v6i8.29>
27. Vsdna NS, Muniappan M, Kannan I, Viswanathan S. Phytochemical analysis and docking study of compounds present in a polyherbal preparation used in the treatment of dermatophytosis. *Curr. Med. Myc.* 2017; 3(4):6. <https://doi.org/10.29252/cmm.3.4.6>
28. Price E, Weinheimer M, Rivkin A, Jenkins G, Nijssen M, Cox PB, DeGoeij D. Beyond Rule of Five and PROTACs in Modern Drug Discovery: Polarity Reducers, Chameleonicity, and the Evolving Physicochemical Landscape. *J. Med. Chem.* 2024; 67(7):5683-5698. <https://doi.org/10.1021/acs.jmedchem.3c02332>

29. Daina A, Michielin O, Zoete V. SwissADME: a free web tool to evaluate pharmacokinetics, drug-likeness and medicinal chemistry friendliness of small molecules. *Sci. Rep.* 2017; 7(1):42717. <https://doi.org/10.1038/srep42717>
30. Durán-Iturbide NA, Díaz-Eufracio BI, Medina-Franco JL. In silico ADME/Tox profiling of natural products: A focus on BIOFACQUIM. *ACS omega.* 2020; 5(26):16076-16084. <https://doi.org/10.1021/acsomega.0c01581>
31. Abdulrahman HL, Uzairu A, Uba S. Computational pharmacokinetic analysis on some newly designed 2-anilinopyrimidine derivative compounds as anti-triple-negative breast cancer drug compounds. *Bull. Nat. Res. Cen.* 2020; 44:1-8. <https://doi.org/10.1186/s42269-020-00321-z>
32. Abouzied AS, Abd-Rabo MM, Huwaimel B, Almahmoud SA, Almarshdi AA, Alharbi FM, Alenzi SS, Alshar BN, Alafnan A. In silico pharmacokinetic profiling of the identified bioactive metabolites of *Pergularia tomentosa* L. Latex extract and *in vitro* cytotoxic activity via the induction of caspase-dependent apoptosis with s-phase arrest. *Pharmaceuticals.* 2022; 15(9):1132. <https://doi.org/10.3390/ph15091132>
33. Loiseau A, Asila V, Boitel-Aullen G, Lam M, Salmain M, Boujday S. Silver-based plasmonic nanoparticles for and their use in biosensing. *Biosensors.* 2019; 9(2):78. <https://doi.org/10.3390/bios9020078>
34. Chowdhury S, Yusof F, Faruck MO, Sulaiman N. Process optimisation of silver nanoparticle synthesis using response surface methodology. *Proc. Eng.* 2016; 148:992-999. <https://doi.org/10.1016/j.proeng.2016.06.552>
35. Schiller H, Young C, Schulze S, Tripepi M, Pohlschroder M. A twist to the Kirby-Bauer disk diffusion susceptibility test: an accessible laboratory experiment comparing *Haloflex volcanii* and *Escherichia coli* antibiotic susceptibility to highlight the unique cell biology of archaea. *J. Microbio. Bio. Edu.* 2022; 23(1):e00234-21. <https://doi.org/10.1128/jmbe.00234-21>
36. Aponjolosun SB, Fasola RT. Phytochemical, antimicrobial, and toxicity evaluation of *Anacardium occidentale* Linn. leaf extracts. *Trop J. Pharm Res.* 2022; 4(4):113-122. <https://doi.org/10.26538/tjnpr/v4i4.1>
37. Usman SO, Aliyu AA, Sowemimo AA, Sofidiya MO. Anti-Inflammatory Investigations of the Ethanol Extract of *Phaulopsis falcisepala* CB Clarke (Acanthaceae) Whole Plant in Rodents. *Trop J. Pharm Res.* 2019; 4(4):165-171. <https://doi.org/10.26538/tjnpr/v4i4.8>
38. Li H, Komori A, Li M, Chen X, Yang AW, Sun X, Liu Y, Hung A, Zhao X, Zhou L. Multi-ligand molecular docking, simulation, free energy calculations and wavelet analysis of the synergistic effects between natural compounds baicalein and cubebin for the inhibition of the main protease of SARS-CoV-2. *J. Mole. Liq.* 2023; 374:121253. <https://doi.org/10.1016/j.molliq.2023.121253>
39. Basu A, Sarkar A, Maulik U. Molecular docking study of potential phytochemicals and their effects on the complex of SARS-CoV2 spike protein and human ACE2. *Sci. Rep.* 2020; 10(1):17699. <https://doi.org/10.1038/s41598-020-74715-4>
40. Adi PJ, Yellapu NK, Matcha B. Modeling, molecular docking, probing catalytic binding mode of acetyl-CoA malate synthase G in *Brucella melitensis* 16M. *Biochem. Biophys. Rep.* 2016; 8:192-199. <https://doi.org/10.1016/j.bbrep.2016.08.020>
41. Al Mogren MM, Zerroug E, Belaidi S, BenAmor A, Al Harbi SD. Molecular structure, drug-likeness, and QSAR modelling of 1, 2-diazole derivatives as inhibitors of enoyl-acyl carrier protein reductase. *J. King Saud Uni.-Sc.* 2020; 32(4):2301-2310. <https://doi.org/10.1016/j.jksus.2020.03.007>
42. Bitew M, Desalegn T, Demissie TB, Belayneh A, Endale M, Eswaramoorthy R. Pharmacokinetics and drug-likeness of antidiabetic flavonoids: Molecular docking and DFT study. *PLoS One.* 2021; 16(12):e0260853. <https://doi.org/10.1371/journal.pone.0260853>
43. Jia CY, Li JY, Hao GF, Yang GF. A drug-likeness toolbox facilitates ADMET study in drug discovery. *Drug Disc. Tod.* 2020; 25(1):248-258. <https://doi.org/10.1016/j.drudis.2019.10.014>
44. Ammar O. In silico pharmacodynamics, toxicity profile and biological activities of the Saharan medicinal plant *Limoniastrum feei*. *Braz. J. Pharm. Sci.* 2017; 53(03):e00061. <https://doi.org/10.1590/s2175-97902017000300061>
45. Malik A, Afaq S, El Gamal B, Abd Ellatif M, Hassan WN, Dera A, Noor R, Tarique M. Molecular docking and pharmacokinetic evaluation of natural compounds as targeted inhibitors against Crz1 protein in *Rhizoctonia solani*. *Bioinfor.* 2019; 15(4):277. <https://doi.org/10.6026/97320630015277>
46. Aina OS, Rofiu MO, Oloba-Whenu OA, Olasupo IA, Adams LA, Familoni OB. Drug design and *in-silico* study of 2-alkoxylatedquinoline-3-carbaldehyde compounds: Inhibitors of *Mycobacterium tuberculosis*. *Sci. Afr.* 2024; 23:e01985. <https://doi.org/10.1016/j.sciaf.2023.e01985>
47. Oomariyah N, van Dijk G. The bioavailability prediction and screening phytochemicals of *Sansevieria trifasciata* leaves extract. *InMATEC Web of Conf.* 2022; 372:02003. EDP Sci. <https://doi.org/10.1051/mateconf/202237202003>
48. Taj G. Characterization of Phytochemical Inhibitors of the COVID-19 Primary Protease Using Molecular Modelling Approach. *Asi. J. Microbio. Biotech.* 2024; 9(2):60-69. <https://doi.org/10.56557/ajmab/2024/v9i28800>